Solid State Phenomena Vol 228 (2015) pp 394-409 *Online: 2015-03-30*
© (2015) Trans Tech Publications, Switzerland
doi:10.4028/www.scientific.net/SSP.228.394

On the Use of the Scanning Electrochemical Microscopy in Corrosion Research

B. Łosiewicz[a], M. Popczyk[b], A. Smołka[c], M. Szklarska[d], P. Osak[e], A. Budniok[f]

Silesian Interdisciplinary Centre for Education and Research, University of Silesia, ul. 75 Pułku Piechoty 1, 41-500 Chorzów, Poland

[a]bozena.losiewicz@us.edu.pl, [b]magdalena.popczyk@us.edu.pl, [c]mszklarska@us.edu.pl,

[d]agnieszka.smolka@us.edu.pl, [e]posak@us.edu.pl, [f]antoni.budniok@us.edu.pl

Keywords: Corrosion test, electrochemical technique, scanning electrochemical microscopy.

Abstract. This paper deals with the basic theory and the usability of Scanning Electrochemical Microscopy (SECM) in corrosion research. The SECM is the *in situ* method of surface characterization which is based on the scanning of the tested surface using ultramicroelectrode and simultaneous electrochemical testing of the surface. This technique provides an electrochemical imaging of the surface. Key applications of SECM have been demonstrated based on the newest literature data covering the past two years of the active research in the field of corrosion in a nanoscale.

Introduction

Spectroscopic methods of surface analysis (XPS, AES, UPS, SIMS, LMMS and EM) consist in the removal of the sample from the corrosive solution and placing it in a high vacuum in order to perform the analysis of the surface. The disadvantage of this method is the fact that during the transfer of the sample from the solution into the spectometer chamber profound chemical and structural changes may occur on its surface. The scanning electrochemical microscopy (SECM) method of surface testing described in this paper is the *in situ* method. Therefore the surface of the material is tested during interaction with the aggressive environment. Fig. 1 shows that number of publications per year related to SECM dynamically increased from 11 publications in 1994 to 121 publications in 2013.

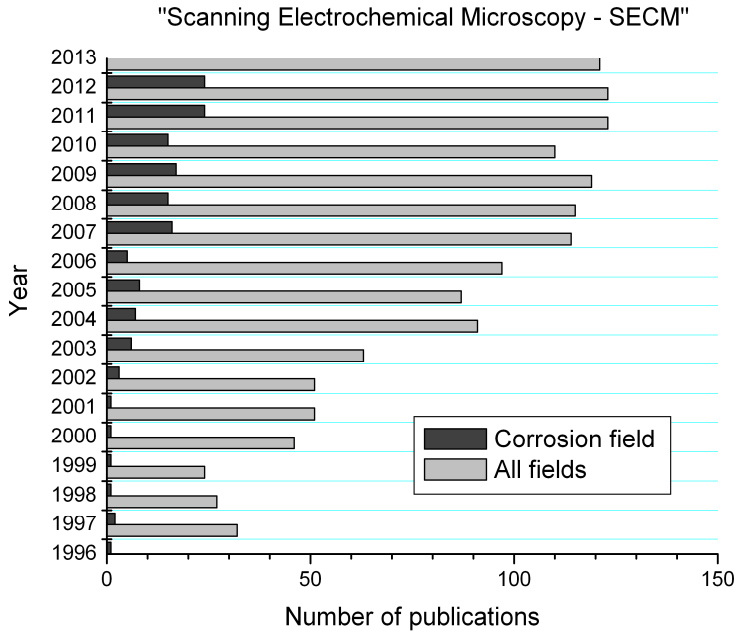

Fig. 1. Number of publications per year related to SECM. Data collected from the Science Direct. Keywords for search: “Scanning Electrochemical Microscopy”.

A significant part of publications covering the time from 1994 (3 publications) to 2013 (26 publications) indicates the intensive development of SECM for the study of phenomena related to corrosion (Fig. 1). As it is shown in this review work, exciting new developments are currently emerging according to possibility of application of SECM for localized corrosion evaluation [1-38]. Key results have been extracted from recent publications covering the past two years of research activity in this field.

Theory

Scanning electrochemical microscopy (SECM) is a scanning probe microscopy (SPM) the diagram of which is presented in Fig. 2.

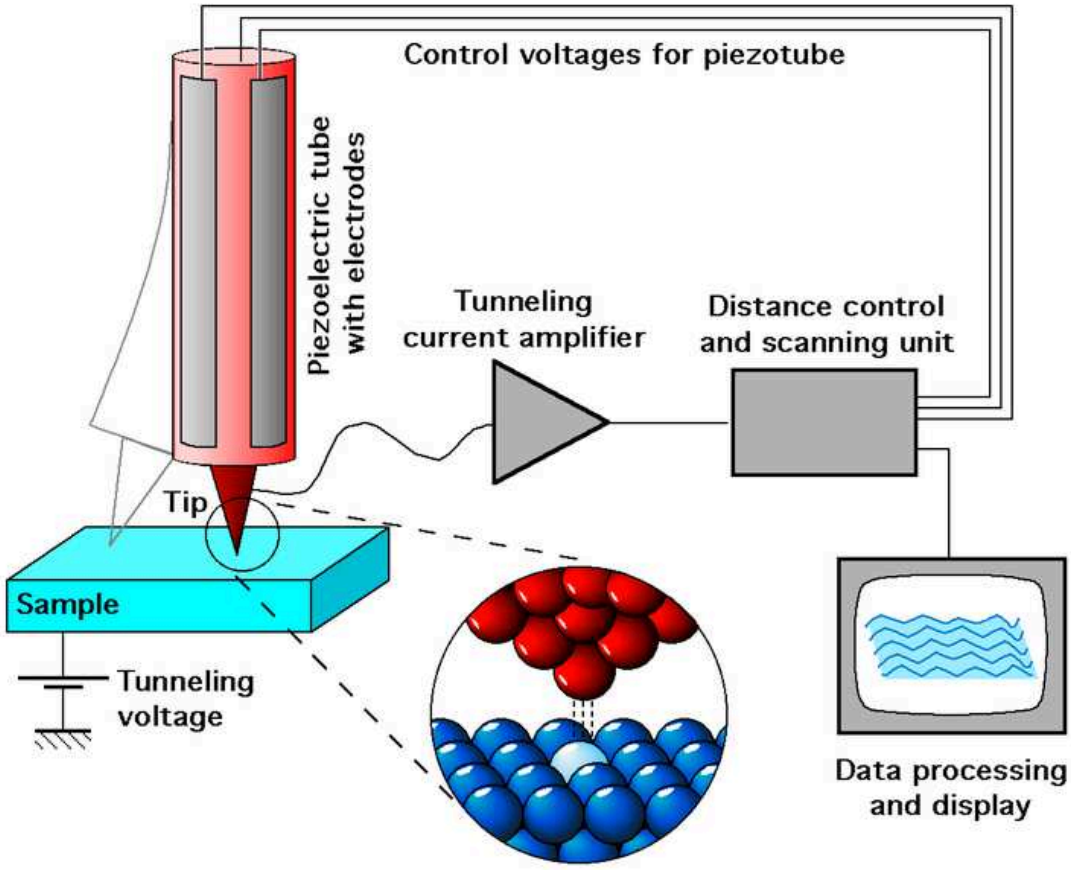

Fig. 2. Diagram of a microscope with a scanning probe (SPM) [2].

However, SECM measuring system consists of an electrolytic dish with a set of electrodes: the tested one (*Substrate*), the supporting one (*Auxiliary*), the referential one (*Reference*) and the probe, i.e. the indicator electrode (*Tip*), the piezoelectric manipulators and an appropriately constructed biopotentiostat coupled with the computer. The indicator electrode is connected to the bipotentiostat designed to work with the microelectrodes. An overview diagram of the SECM measurement system is shown in Fig. 3.

The main mechanical part is an $x - y$ table precisely actuated by micrometer screw driven gears connected to stepper motors. A computer equipped with appropriate software controls the mechanical and electronic parts of the measuring set while the camera allows one to track the topographical image of the tested sample surface.

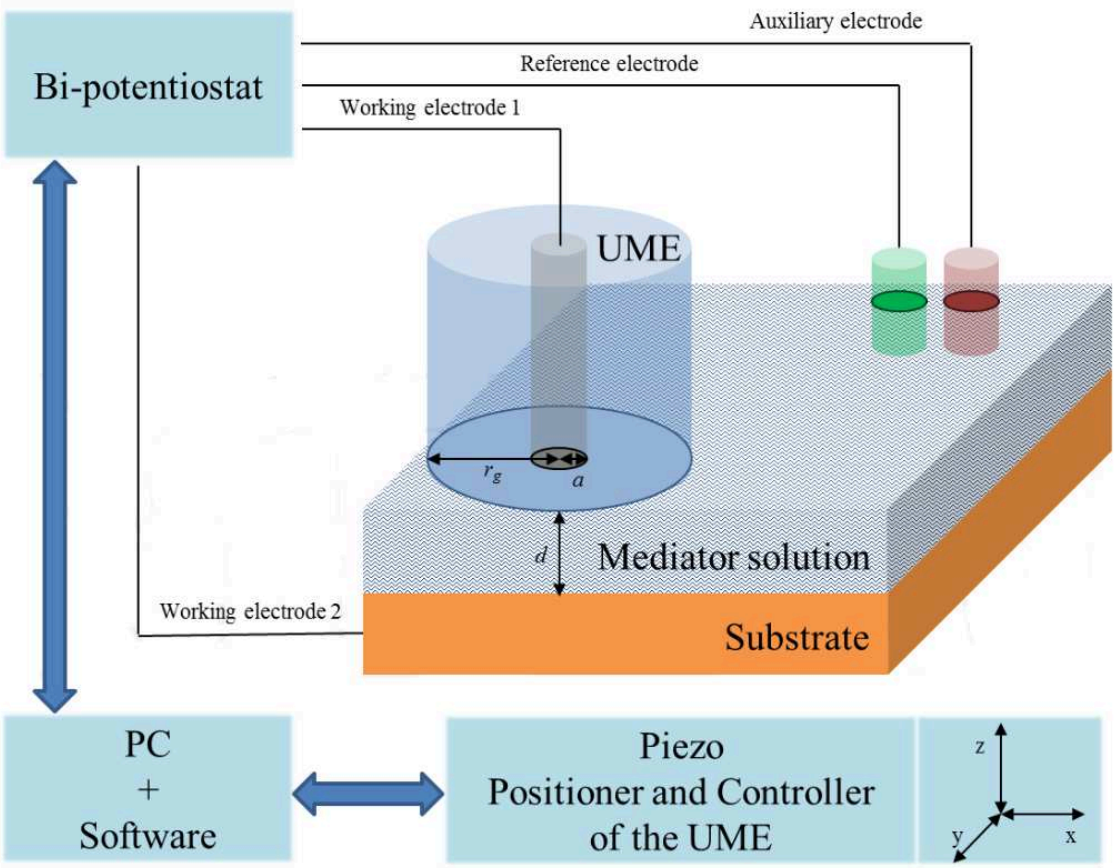

a)

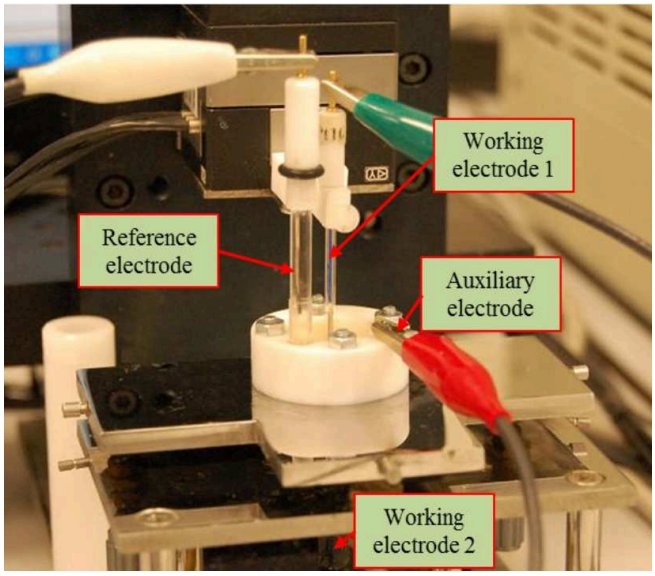

b)

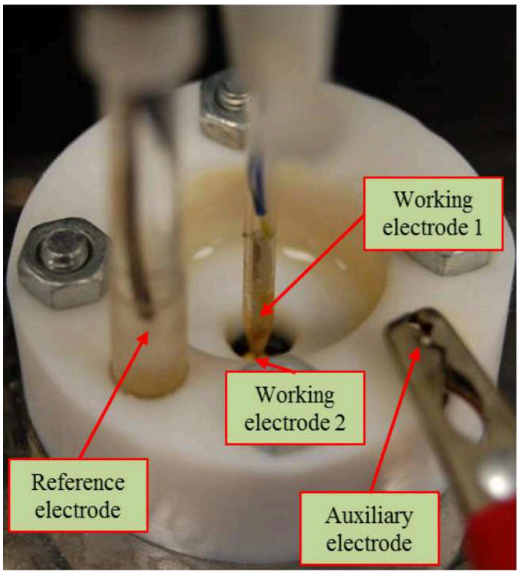

c)

Fig. 3. a) Block diagram of the SECM measurement set, b) real picture of the ChInstruments 920D measurement apparatus using the SECM, and c) the detailed image of the electrochemical cell with four-electrode configuration [34].

A high input resistance ultramicroelectrode (UME) combined with a movable part of the table is shifted by the 300 nm step in relation to the fixed test electrode. The probe (an indicator electrode) is presented in Fig. 4.

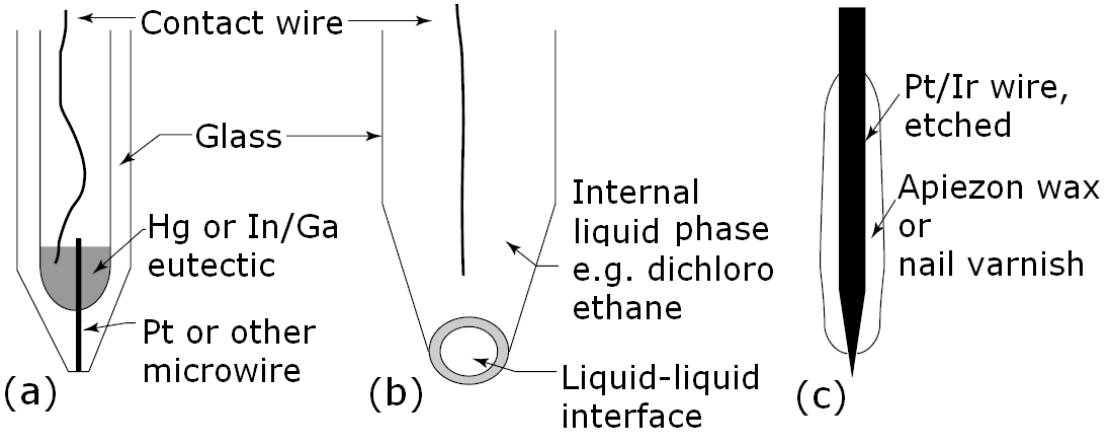

Fig. 4. Indicator electrode - SECM tips: a) standard voltammetric microdisk (for $r_o \geq 0.6$ μm), b) micropipette (all r_o), and c) etched metal tip (for $r_o < 1$ μm) [36].

The current (or the potential) related to the redox processes taking place on this electrode in registered on the metal blade of the probe (the needle), (usually made of Pt, Au, carbon fiber, etc.). The ideal and real probe is shown in Fig. 5.

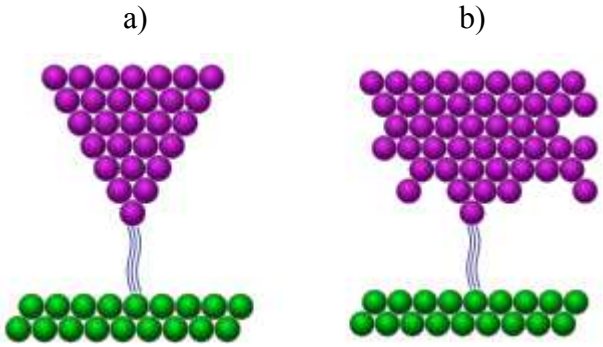

Fig. 5. a) Ideal needle, and b) real needle.

The precise horizontal shift of the probe and bringing the probe closer to the surface is carried out by means of piezoelectric manipulators and an optical microscope. Preparing a sharp end on the wire with micrometers in diameter requires extraordinary precision and is usually done using the electrolytic etching methods. The radius of the indicator electrode is usually a = 1-25 μm, and the distance between the surface of the blade (d) is usually 3-6 times greater than the radius of the indicator electrode. The blade of the probe may be gradually brought closer to a desired test surface of the microsite (even at the distance shorter than a) with the current pulse being simultaneously recorded. Current density dependence on the probe from its distance from the surface is called an approach curve. The shape of the approach curve (presented below) provides for clear determination whether the analyzed microsite conducts electricity, or whether it is an insulator. The space between the test sample and the probe is filled by an appropriately selected electrolytic environment which makes it possible to track the changes in the electrochemical parameters of the set while the probe moves in a given direction. An important role during testing of the probe

surface is played by the so called feedback, the presence of which should be identified with the flow of Faraday's current between the probe and the test sample. If the electrodes are immersed in the solution with a reduced form (redox mediator, R) and with a suitably chosen UME positive potential, the mediator diffusing from the depths of the solution enters into a reaction according to the following equation:

$$R - e^- \leftrightarrow O. \quad (1)$$

If the indicator electrode is placed quite far away from the surface of the test electrode (substrate), then the current flows in a circuit, which is described as follows:

$$i_{T,\infty} = 4\,n\,F\,D\,c\,a, \quad (2)$$

where n is the number of electrons, F – Faraday's constant, D – diffusion coefficient of the mediator, c – concentration of the reduced form, R and a – radius of the ultramicroelectrode.

After some time, the reaction (1) reaches a steady state and the current reaches a maximum constant value of $i_{T,\infty}$. After reversing the direction of the electrode polarization the reaction (1) goes in the opposite direction. Thus, a current-voltage sigmoidal-shaped cyclic curve is obtained (Fig. 6).

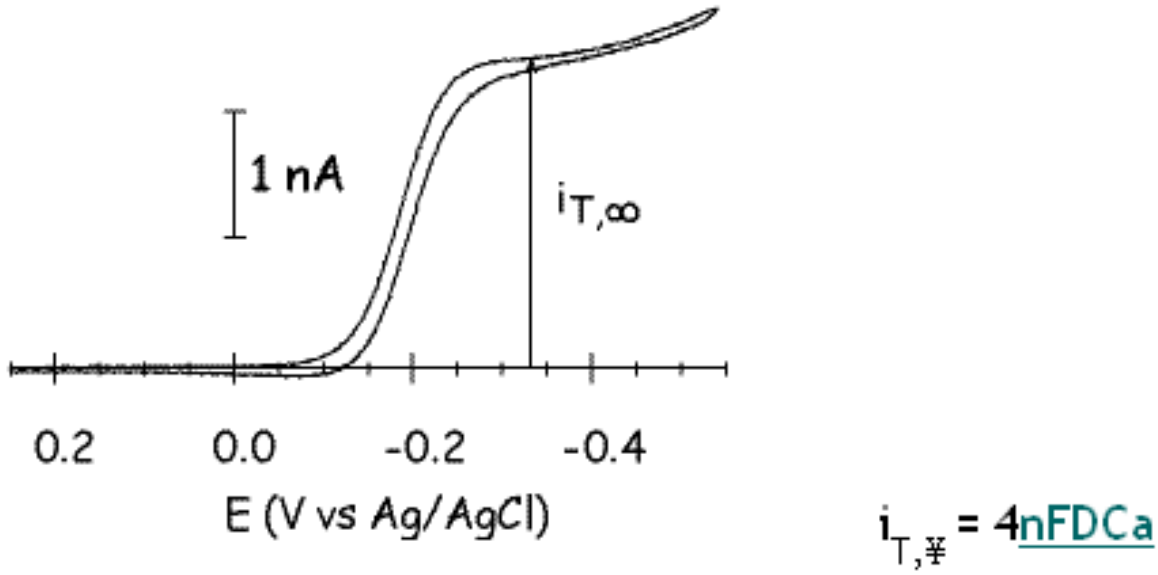

Fig. 6. Voltamperometric cyclic curve for the $[Ru(NH_3)_6]^{3+}$ ion obtained in a steady state on a platinum ultramikcoelectrode [35].

If the indicator electrode is close enough to the surface of the test electrode, then the equilibrium of reaction (1) will be disturbed as a result of increasing concentration of form O developed on the surface of the test electrode (reaction 1). The mediator oxidized form obtained as a result of diffusion reaches the surface of the indicator electrode and is transformed into a reduced form (Figs. 7a-c).

As a result of this process the current value on the surface of the indicator electrode will increase. Thus: $i_T > i_{T,\infty}$, (Fig. 8). Therefore, the closer the indicator electrode to the surface of the test electrode, the greater the value of the recorded current. The observed phenomenon is called positive feedback and is characteristic of conductive test samples.

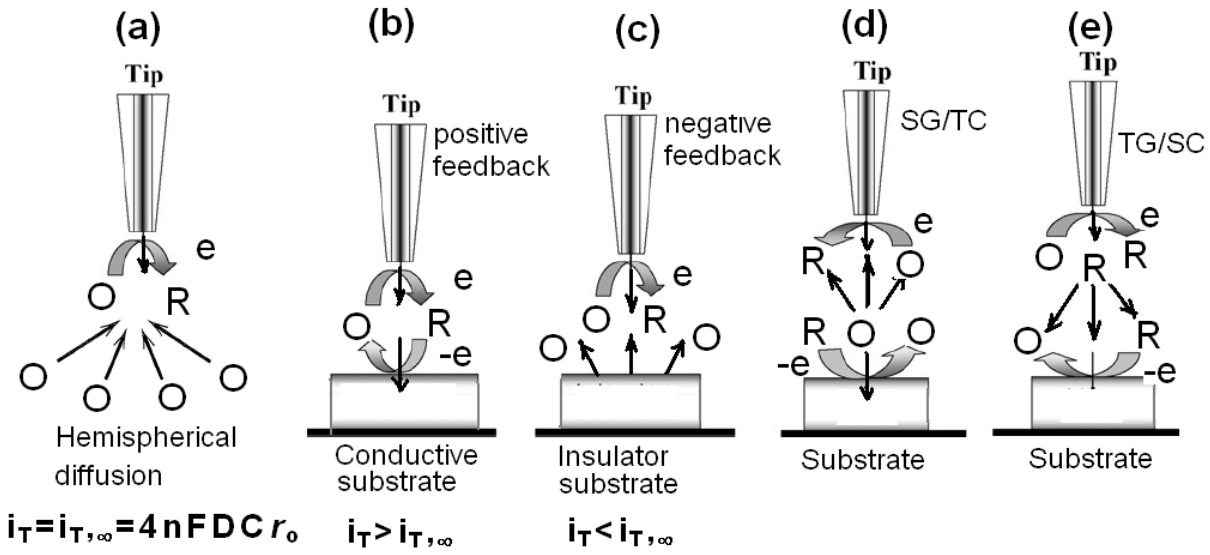

Fig. 7. Basic operational modes of the SECM: a) disc microelectrode tip positioned in the bulk solution (distance of tip from substrate: $d = \infty$) where the steady state tip current (i_T) for the reduction of O into R is totally diffusion controlled, b) the positive feedback mode at a conductive substrate which regenerates O from R, c) the negative feedback mode based on hindered diffusion of O by an insulating substrate, d) substrate generation/tip collection (SG/TC) mode, e) tip generation/substrate collection (TG/SC) mode [36].

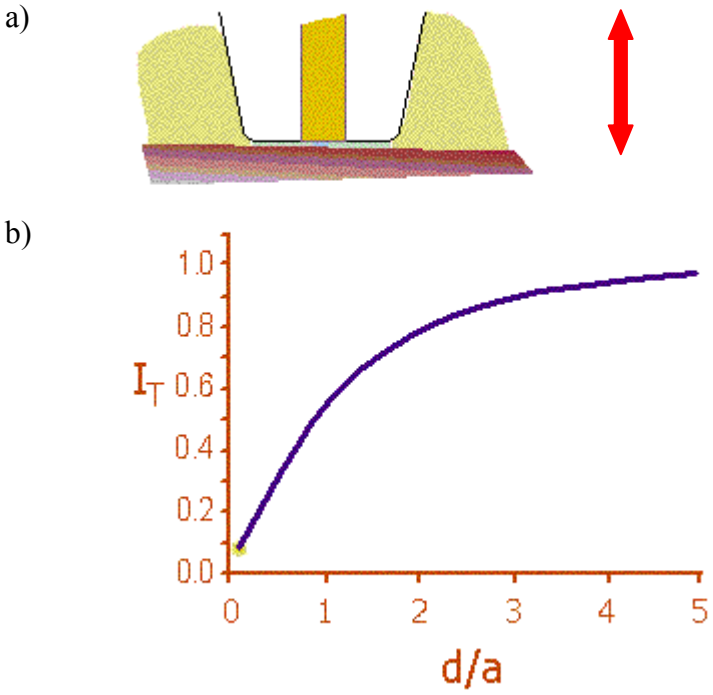

Fig. 8. a) Direction of the probe relocation, b) approach curve for positive feedback (d – distance between the indicator electrode and the test electrode, a – ultramicroelectrode radius) [35].

If, however, the test electrode is not electrically conductive, then reaction (1) takes place only on the surface of the indicator electrode. Therefore, the changes in the voltage of the current can be written as follows: $i_T < i_{T,\infty}$. In this case, there appears negative feedback (Fig. 9). The closer

the indicator electrode to the surface of the test electrode, the lower the intensity of the resulting current.

It is possible, of course, to obtain a transitional state due to partial conductivity of the test electrode, which is characteristic of the corrosive samples or the ones covered with other substances, namely inhibitors. Then, the approach curves are obtained. Their course depends on the degree of the test electrode electric conductivity.

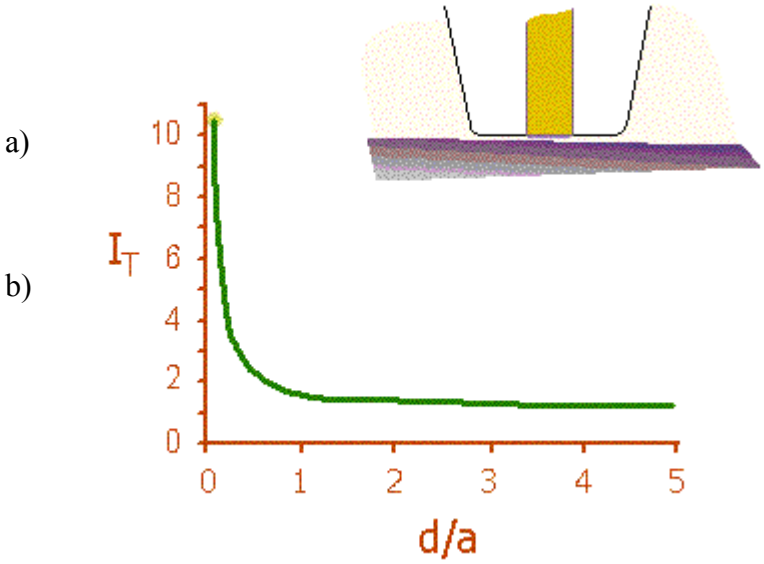

Fig. 9. a) Direction of probe relocation, b) approach curve for negative feedback (*d* – distance between the indicator electrode and the surface of the test electrode, *a* – ultramicroelectrode radius) [35].

Both UME and the test electrode can be used as indicator electrodes in the four-electrode scanning electrochemical microscopy. Therefore, the product of the electrode reaction can be generated on one of them and collected on the other (generating/collection mode, G/C). Therefore, there are two possible options for the G/C of the microscope. The first one consists in generating the product on the surface of the and test electrode test and its accumulation on the indicator electrode, the SG/TC (substrate generation/tip collection), Fig. 7c and vice versa, TC/SG (collection tip substrate generation), Fig. 7d. It must be noted that the G/C method is very sensitive because the background signal is very weak. Therefore, this method is used for testing the so-called concentration profiles of different electroactive substances produced on the electrodes thereby for examining the kinetics and the mechanism of complex electrode reactions. These include electrochemical corrosion tests, electrochemical deposition (nucleation) and an increase in deposits of the local corrosion of passivating metals, the impact of surfactants on corrosion processes and the measurement of the properties of passive semiconductor films. With the use of microelectrodes sensitive to a specific product of an electrode reaction (ISE) one can obtain distribution maps of this product on the surface of the test electrode. In addition, by applying changeable voltage of different frequencies between a mobile indicator electrode (the tip) and a test electrode (the substrate) and recording the current response, one can measure local impedance.

Scanning with a probe (an indicator electrode) over the test surface in the *x*–*y* plane makes it possible to draw the topography of a surface (i.e. the surface map). On such a surface map sites with specific reactivity can be easily recorded.

There are two ways to scan the surface of the test electrode:

1. constant height method (CHM)
2. constant gap mode (CGM).

In the first case the probe moves at a constant height over the surface of the test sample and i_T current changes within the function of the distance between the tip and the sample surface are registered. This solution can only be applied in the case of samples with flat surface or when using thick scanning tips. Scanning of the protuberances on the surface can cause damage to the tip, whereas concavities cause that the image of the sample is blurred or disappears completely.

The second solution (more complex) is much better because the tip can move away or get closer to the surface of the test sample depending on the shape of the surface. Determining an appropriate distance between the tip and the test sample is possible thanks to the use of negative feedback (distance – current – voltage adjusting the height of the tip) which is fast enough. Thus, the collision of the tip with the surface of the test sample can be avoided, and the resulting has good resolution.

Particularly valuable information concerning the kinetics and homo- and heterogeneous processes occurring in close proximity to the surface can be obtained by means of SECM. For this purpose, the so called *redox mediator* is often used. It is in the form of an additive to the test electrolyte of the redox couple such as I / I_3^-. The products of digestion of inclusions permeate into the solution and disturb the balance of the redox mediator. With voltamperometric methods one can assess the type of product, its area of influence and the time needed for its production.
SECM helped determine that as a result of sulfide inclusions (MnS) in stainless steel with acidified chloride solution HS- and $S_2O_3^{2-}$ ions are formed as indirect products of corrosion. The size and shape of individual inclusions can also be determined using SECM. Scanning electrochemical microscopy proved to be useful in determining the products of the impact of the metal substrate modified with a conducting polymer (polypyrrole) and an electrolytic solution.

Use of the SECM in corrosion research

Application of SECM to study of the role of TiO_2 doping on RuO_2-coated electrodes for water oxidation reaction

Recently, Näslund *et al.* [26] applied SECM to investigate novel electrode materials which were obtained by modification of dimensionally stable anodes (DSA) based on the electrocatalytic active RuO_2, conventionally utilized in industry for electrochemical water splitting into hydrogen and oxygen.

To decrease the energy barrier of this process connected with high overpotential required at the anode and to improve the resistance against corrosion, incorporation of TiO_2 into the RuO_2-coated electrodes was proposed. SECM substrate generation – tip collection (SG/TC) imaging results in Fig. 11 show the three different coating zones of mixed $(Ru_{0.76}:Ti_{0.24})O_2$ (left), TiO_2 (middle), and the RuO_2 (right) applied on the Ti sheet. The lower panel in Fig. 11 presents the SECM SG/TC image registered in a situation when the gold UME tip was sensing the electrochemical activity as it was scanned over the surface of the sample under study. Places where the oxygen evolution reaction (OER) occured on the electrode surface, were revealed.

Fig. 12a presents comparison between the SECM SG/TC image and the crack pattern observed by the optical microscope. One can see the enhanced OER electrochemical activity at the places corresponding to the cracks in the RuO_2 coating. Fig. 12b shows the current profile at SECM, indicated with an arrow in the SECM image in Fig. 12a, compared with the crack location.

Based on the obtained SECM SG/TC image registered using a gold UME tip for sensing the oxygen evolution proceeding on pure RuO_2 and TiO_2-doped RuO_2-coated electrodes revealed the higher values of the average current and more evenly distributed electrocatalytic activity for water oxidation on the mixed $(Ru_{1-x}:Ti_x)O_2$-coated electrode where Ru:Ti surface composition was ≅ 50:50 in comparison to that observed on the pure RuO_2-coated electrode.

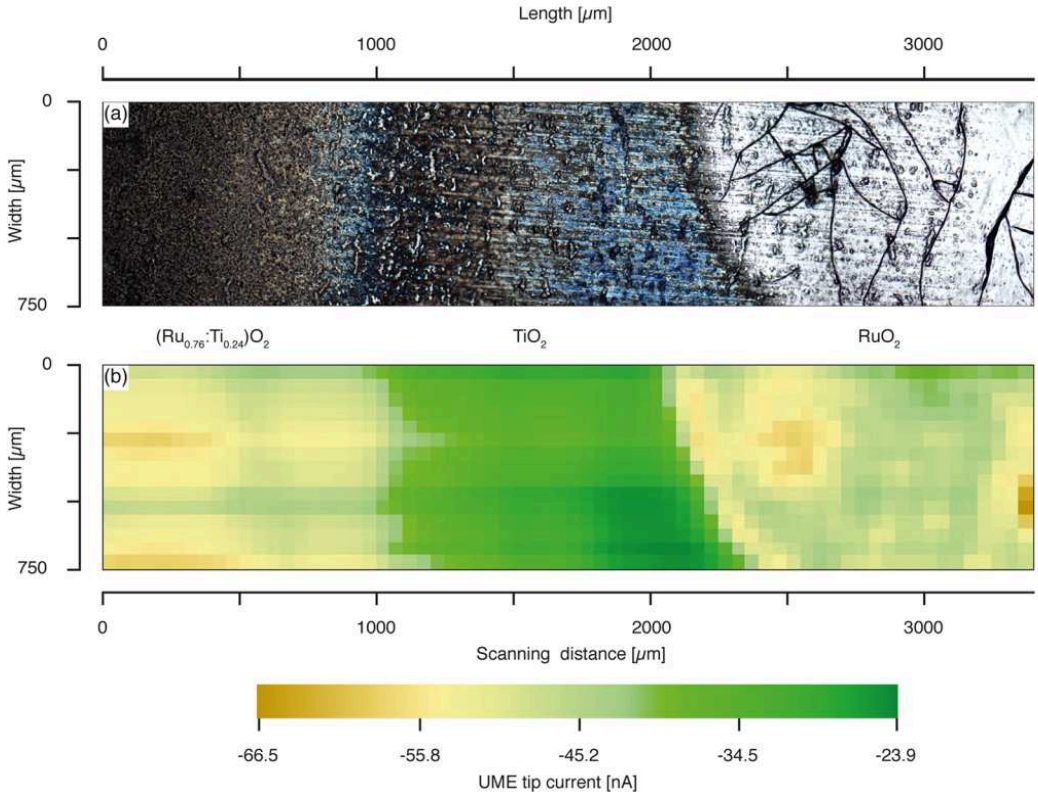

Fig. 11. a) Optical microscopy and b) SECM are shown in the upper and lower panel. The SECM SG/TC impage shows the UME tip current registered for the OER activity on the substrate electrode composed of the two oxide coatings $(Ru_{0.76}:Ti_{0.24})O_2$ and RuO_2 separated by TiO_2, simultaneously [26].

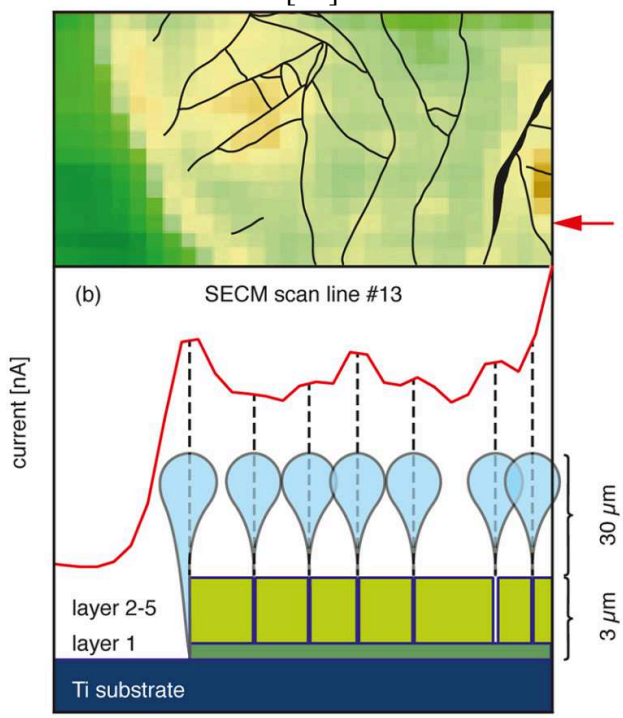

Fig. 12. a) Comparison of the SECM image and the crack pattern observed using the optical microscope image reveals the enhanced OER activity at the cracks in the RuO_2 coating, and b) the current profile at SECM scan no. 13, indicated with an arrow in the SECM image in Fig. 12a, compared with the crack location. Despite the small width of the cracks from 5 to 15 μm, the plume of oxygen gas leaving the cracks in the RuO_2 coating will have a size being comparable with a diameter of the UME of 100 μm [26].

Moreover, the authors proved based on the optical microscope and the SECM images, that on the pure RuO_2-coated electrode, regions of higher electrocatalytic activity with visible crack pattern, were detected. It was suggested that the higher electrochemical activity at the cracks which was examined successfully by the SG/TC mode of SECM, was connected with TiO_2-doping in the first applied layer of RuO_2 due to diffusion of Ti from the Ti sheet served as a support.

Application of SECM to detection and quantification of hydrogen fluxes from a corroding magnesium alloy

Local flux of hydrogen from the industrial AM50 die-cast alloy corrosion was investigated using SG/TP SECM by Tefashe *et al.* [11]. The microstructure of this alloy consists of primary α-Mg grains along with a network of partially or fully divorced mixture of intermetallic β-$Mg_{17}Al_{12}$ and eutectic Mg. Intermetallic phases of the Al-Mn system were also present in such a microstructure. During galvanic corrosion of magnesium in aqueous solutions $Mg(OH)_2$ and H_2 are produced. It was observed that in sodium chloride solutions Mg is readily oxidized when galvanically coupled with other metals. On the AM50 alloy after immersion in aqueous solution, microgalvanic couples between the bulk Mg (noted as α in Fig. 13) and the network of eutectic mixture of the intermetallic β-$Mg_{17}Al_{12}$ and Mg, Al-Mn intermetallic phases or Fe-containing inclusions, which were reffered as β in Fig. 13.

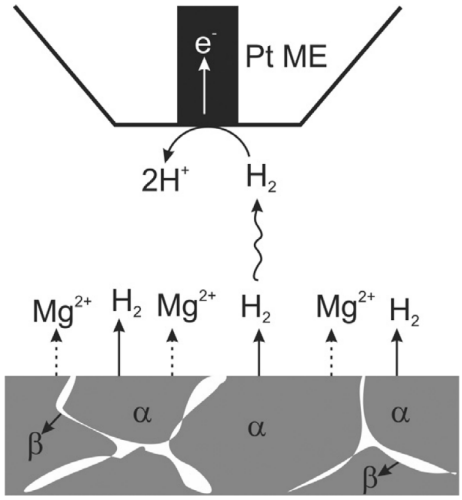

Fig. 13. Scheme of processes considered in SECM investigation of the aqueous H_2 detection during Mg alloy corrosion for an active surface [11].

At the beginning of corrosion process, the α-Mg matrix behavior is typical for the anode with the release of Mg^{2+}, while molecular hydrogen is evoluted at the β cathodic sites. It was reported that direct monitoring of H_2 or H^+ fluxes and performing quantitative studies using SECM is difficult during the corrosion of Mg alloy, because of the presence of a limited experimental window in terms of corrosive solutions and time that is devoid of significant convection effects which originate from hydrogen gas evolution and topographical deviations. However, the investigators found in this work experimental conditions of 0.6 M NaCl solution and exposure time below 60 min under which using SG/TC mode of SECM, monitoring of the local flux of hydrogen evolution at the surface of Mg was possible.

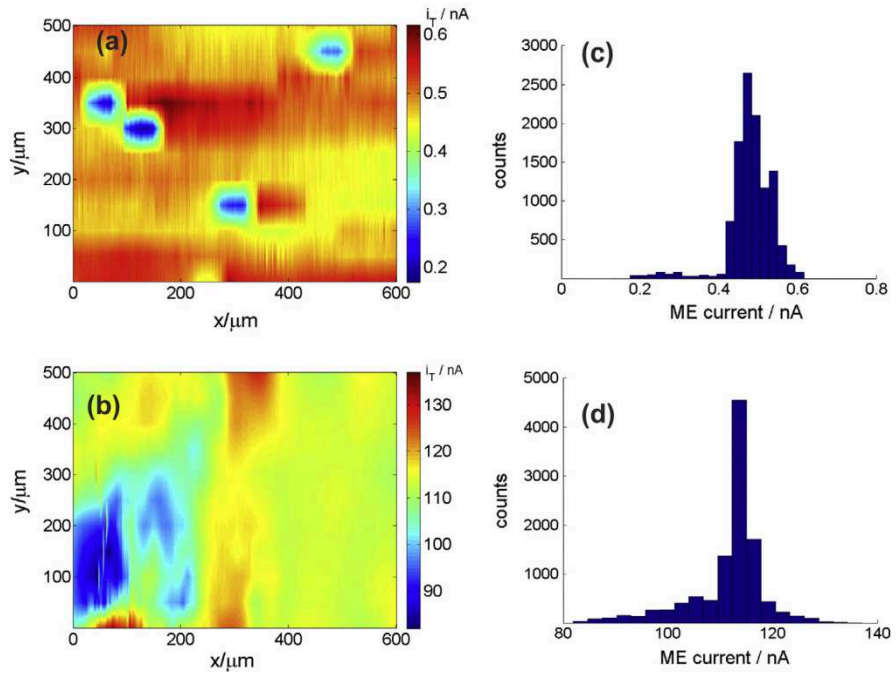

Fig. 14. SECM maps showing H_2 fluxes from the die-cast AM50 alloy after immersion in a 0.6 M NaCl electrolyte for: a) 5 min, and b) 1 h, and c), d) the appropriate histograms of the current distribution extracted from the SECM maps shown in Figs. 14 a and b [11].

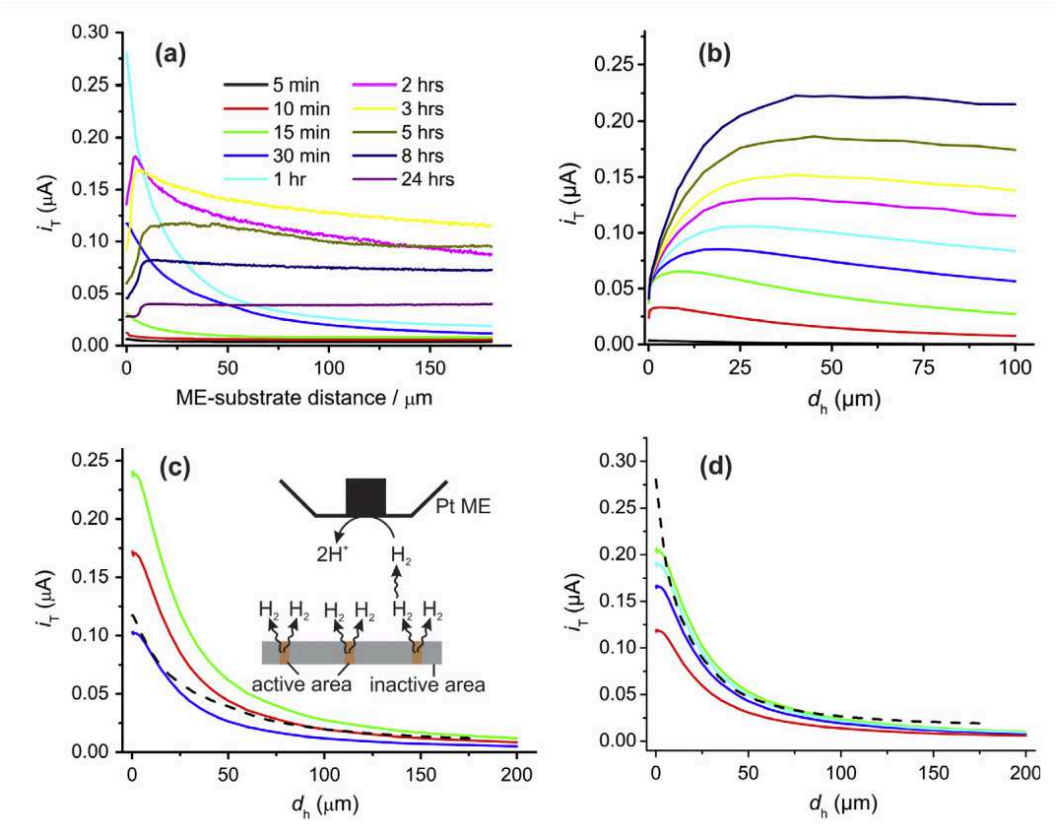

Fig. 15. a) Experimental SECM approach curves for a corroding die-cast AM50 Mg alloy sample for the detection of dissolved H_2 after different immersion times, b) simulated approach curves for a 25 μm diameter Pt ME over active sites of different sizes producing a H_2 flux of 0.7 mmol m^{-2} s^{-1}. Comparison of experimental approach curves marked as dashed lines and simulated approach curves marked as solid lines for time of immersion: c) 30 min and d) 1 h [11].

The authors imaged the variation in H_2 fluxes revealing the time-dependent reaction of corrosion. To monitore and quantify the *in situ* release of hydrogen produced at the β region and intermetallic cathodic sites of the AM50, a platinum microelectrode (ME), was applied. Taking into account that one mole of corroding Mg is accompanied by the evolution of one mole of H_2, a direct comparison of the detected hydrogen at the ME to the rate of occuring corrosion was carried out.

The authors obtained SECM maps (Fig. 14) and multiple SECM approach curves (Fig. 15) which allowed to make observations of the time-dependent change of the AM50 alloy surface. The registered approach curves were compared to a numerical model to evaluate the magnitude of the H_2 flux as the active size of hydrogen producing features increased [11].

Application of SECM to study of interfacial barrier properties of TiO_2 nanotube arrays

Three generations of TiO_2 nanotubular arrays obtained by anodization of titanium foil (TiNT) in: (*i*) aqueous acid containing fluoride media, (*ii*) organic based containing fluoride media, and (*iii*) chloride containing electrolyte, were studied using SECM by Aïnouche *et al.* [8]. SEM images of TiO_2 nanotubular oxide layers grown on titanium under different electrochemical conditions are displayed in Fig. 16.

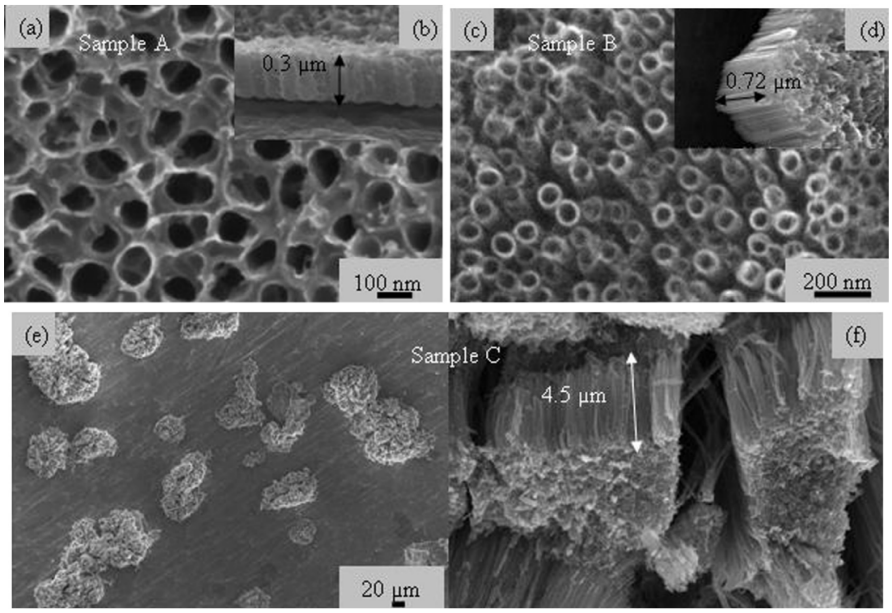

Fig. 16. SEM top and cross-sectional images of TiO_2 nanotubular oxide layers grown on titanium at the anodization potential of 20 V under different electrochemical conditions: Sample A – 1 wt.% HF for 20 min, Sample B – ethylene glycol + 0.3 M NH_4F + 0.2 M H_3PO_4 + 0.15 wt.% H_2O for 120 min, and Sample C – 0.3 M NaCl for 1 min [8].

The authors investigated the effect of the electrolyte composition on barrier layer properties of TiNT. Correlation between the dimensional aspect of TiNT and the electrochemical characteristics was found. Aïnouche *et al.* [8] also discussed semiconducting properties and thickness of TiNT in relation to the electrolyte used for anodization. The authors as first used SECM for in situ characterization of surface chemical activity of titanium in chloride solution. The SECM investigation revealed the initiation of corrosion pits on titanium in 0.3 M NaCl solution at the open circuit potential as well as the surrounding cathodic reaction (Fig. 17). Fig. 17a shows the 3D SECM image for a titanium surface under such conditions with microcells formed on the exposed surface of the sample under study. One can observe numerous anodic and cathodic current peaks being characterized by different levels of the current in different active areas. The authors stated that the current transients represent the break-down of passivity and can be related to the

nucleation process of corrosion pits occuring on the sample surface. As the probable reaction at the tip was assigned the oxidation of Ti^{3+} to Ti^{4+} on the SECM tip. The released Ti^{3+} from the locally dissolved point on the surface is a pit precursor. The investigators also observed that some anodic peaks were succeeded immediately by cathodic peaks, and that both the oxidation and the reduction reactions proceeded simultaneously at local pitting sites on Ti surface.

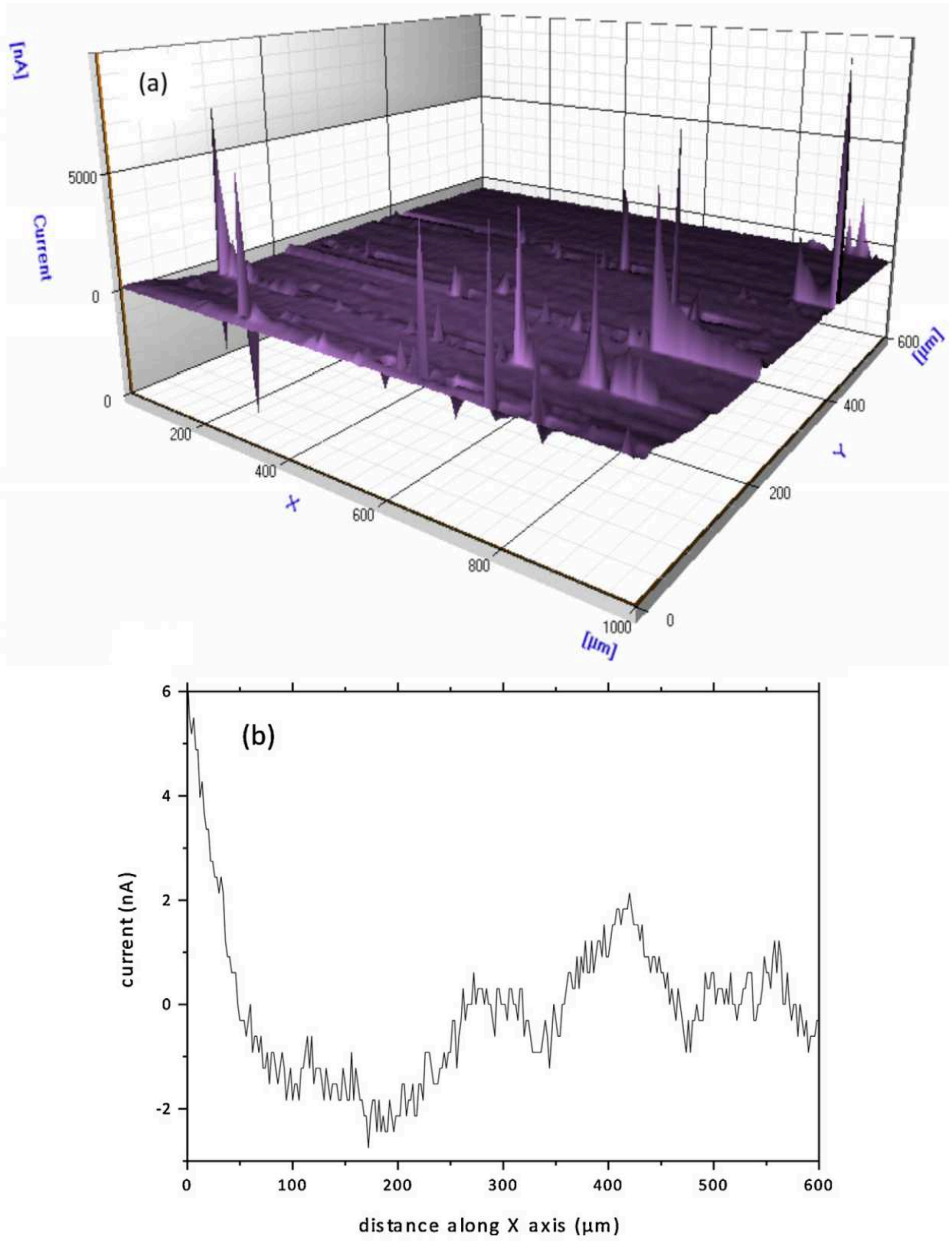

Fig. 17. a) 3D SECM image for a titanium surface in 0.3 M NaCl electrolyte at the open circuit potential, where *x* and *y* axes show an area of 1000 µm by 600 µm, and b) line scan with the positive and negative wings of the tip current which passed over and beyond a pit [8].

Fig. 17b presents a line scan with the positive and negative wings of the tip current which passed over and beyond a pit. Such a behavior is typical for the metal at the open circuit potential and can be ascribed to an indirect detection of the cathodic reaction [8]. According to literature, the negative wing on the probe current corresponds to a reduced background current [37]. It was also shown that far bellow pitting potential, pits may nucleate and propagate there into the metastable

state [38]. It should also be noticed that breakdown occured with the same frequency within the duration interval of tests.

Summary

The SECM employs an UME probe (tip) to induce chemical changes and collect electrochemical information while approaching or scanning the tested surface. This technique requires minimal sample preparation as compared to other spectroscopic techniques. Additional advantage of the SECM is possibility of numerical modelling of the image outputs what allows to obtain information and analysis of the occurred reaction kinetics. The SECM is particularly useful for testing: the microdensity of the anticorrosive galvanic coatings or the ones obtained using paints and as a result of adsorption inhibitors, galvanic anticorrosion, composite materials (mainly with regard to their corrosion resistance), or mechanisms of electrode processes. The SECM can also be used as a complementary method to spectroscopic methods such as XPS, AES and Raman which make it possible to register concentration distribution maps on the surface of the tested sample. The SECM method plays an important role in the research into the deposition of different microstructures which is conducted with the use of a supporting microelectrode. However, the SECM must be installed in a place not exposed to vibrations or shock as they cause numerous faults or damage to the measuring set.

Acknowledgement

M.Sc. M. Szklarska and M.Sc. P. Osak is supported by the Forszt project co-financed by EU from the European Social Fund.

References

[1] R. Leiva-García, R. Sánchez-Tovar, C. Escrivà-Cerdán, J. García-Antón: Role of Modern Localised Electrochemical Techniques to Evaluate the Corrosion on Heterogeneous Surrfaces, Chapter 9, in: Modern Electrochemical Methods in Nano, Surface and Corrosion Science, M. Aliofkhazraei, Ed., Intech, 2014, http://dx.doi.org/10.5772/57204.

[2] http://en.wikipedia.org/wiki/Scanning_tunneling_microscope.

[3] J. Izquierdo, L. Martín-Ruíz, B.M. Fernández-Pérez, R. Rodríguez-Raposo, J.J. Santana: J. Electroanal. Chem. Vol. 728 (2014), p. 148.

[4] J. Izquierdo, G. Bolat, D. Mareci, C. Munteanu, S. González, R.M. Souto: Appl. Surf. Sci. Vol. 313 (2014), p. 259.

[5] D. Sidane, E. Bousquet, O. Devos, M. Puiggali, M. Touzet, V. Vivier: J. Electroanal. Chem. (2014) (article in press), http://dx.doi.org/10.1016/j.jelechem.2014.06.025.

[6] A.R. Zeradjanin, N. Menzel, W. Schuhmann, P. Strasser: Phys. Chem. Chem. Phys. Vol. 16 (2014), p. 13741.

[7] J. Izquierdo, L. Martín-Ruíz, B.M. Fernández-Pérez, L. Fernández-Mérida, J.J. Santana, R.M. Souto: Electrochim. Acta Vol. 134 (2014), p. 167.

[8] L. Aïnouche, L. Hamadou, A. Kadri, N. Benbrahim, D. Bradai: Electrochim. Acta Vol. 133 (2014), p. 597.

[9] W. Liu, F. Cao, Y. Xia, L. Chang, J. Zhang: Electrochim. Acta Vol. 132 (2014), p. 377.

[10] A.S. Bandarenka, A. Maljusch, V. Kuznetsov, K. Eckhard, W. Schuhmann: J. Phys. Chem. C. Vol. 118 (2014), p. 8952.

[11] U.M. Tefashe, M.E. Snowden, P.D. Ducharme, M. Danaie, G.A. Botton, J. Mauzeroll: J. Electroanal. Chem. Vol. 720-721 (2014), p. 121.

[12] N. Esmaeili, J. Neshati, I. Yavari: J. Ind. Eng. Chem. (2014) (article in press), http://dx.doi.org/10.1016/j.jiec.2014.07.004.

[13] C. Li, L. Li, C. Wang, Y. Zhu, W. Zhang: Corros. Sci. Vol. 80 (2014), p. 511.

[14] A. Singh, Y. Lin, W. Liu, S. Yu, J. Pan, C. Ren, D. Kuanhai: J. Ind. Eng. Chem. (2014) (article in press), http://dx.doi.org/10.1016/j.jiec.2014.01.033.

[15] E. Martinez-Lombardia, Y. Gonzalez-Garcia, L. Lapeire, I. De Graeve, K. Verbeken, L. Kestens, J.M.C. Mol, H. Terryn: Electrochim. Acta Vol. 116 (2014), p. 89.

[16] A. Maho, F. Kanoufi, C. Combellas, J. Delhalle, Z. Mekhalif: Electrochim. Acta Vol. 116 (2014), p. 78.

[17] S.S. Jamali, S.E. Moulton, D.E. Tallman, M. Forsyth, J. Weber, G.G. Wallace: Corros. Sci. Vol. 86 (2014), p. 93.

[18] X.J. Raj, T. Nishimura: ISIJ International Vol. 54 (3) (2014), p. 693.

[19] A. Singh, Y. Lin, W. Liu, D. Kuanhai, J. Pan, B. Huang, C. Ren, D. Zeng: J. Taiwan Inst. Chem. E. Vol. 45 (2014), p. 1918.

[20] R. Moreira, M.K. Schütz, M. Libert, B. Tribollet, V. Vivier: Bioelectrochem. Vol. 97 (2014), p. 69.

[21] S. Thomas, I.S. Cole, Y. Gonzalez-Garcia, M. Chen, M. Musameh, JM.C. Mol, H. Terryn, N. Birbilis: J. Appl. Electrochem. Vol. 44 (2014), p. 747.

[22] D. Sidane, M. Touzet, O. Devos, M. Puiggali, J.P. Larivière, J. Guitard: Corros. Sci. 87 (2014), p. 312.

[23] M. Serrapede, G. Denuault, M. Sosna, G.L. Pesce, R.J. Ball: Anal. Chem. Vol. 85 (2013), p. 8341.

[24] M.B. Jensen, D.E. Tallman: J. Solid State Electrochem. Vol. 17 (2013), p. 2999.

[25] R.K. Zhu, B.T. Lu, J.L. Luo, Y.C. Lu: Appl. Surf. Sci. Vol. 270 (2013), p. 755.

[26] L-Å. Näslund, C.M. Sánchez-Sánchez, Á.S. Ingason, J. Bäckström, E. Herrero, J. Rosen, S. Holmin: J. Phys. Chem. C Vol. 117 (2013), p. 6126.

[27] A. Davoodi, J. Pan, C. Leygraf, R. Parvizi, S. Norgren: Mater. Corros. Vol. 64 (3) (2013), p. 195.

[28] J. Izquierdo, L. Nagy, S.Gonzàlez, J.J. Santana, G. Nagy, R.M. Souto: Electrochem. Commun. Vol. 27 (2013), p. 50.

[29] G. Bolat, J. Izquierdo, J.J. Santana, D. Mareci, R.M. Souto: Electrochim. Acta Vol. 88 (2013), p. 447.

[30] R.M. Souto, A. Kiss, J. Izquierdo, L. Nagy, I. Bitter, G. Nagy: Electrochem. Commun. Vol. 26 (2013), p. 25.

[31] J. Izquierdo, L. Nagy, I. Bitter, R.M. Souto, G. Nagy: Electrochim. Acta Vol. 87 (2013), p. 283.

[32] A. Pilbáth, T. Szabó, J. Telegdi, L. Nyikos: Prog. Org. Coat. Vol. 75 (2012), p. 480.

[33] F. Billi, E. Onofre, E. Ebramzadeh, T. Palacios, M.L. Escudero, M.C. Garcia-Alonso: Surf. Coat. Technol. Vol. 212 (2012), p. 134.

[34] D. Hynek, M. Zurek, P. Babula, V. Adam, R. Kizek: Monitoring of the Surface Modification of Nanoparticles by Electrochemical Measurements Using Scanning Electrochemical Microscope, Chapter 6, in: Modern Electrochemical Methods in Nano, Surface and Corrosion Science, Mahmood Aliofkhazraei, INTECH, 2014, pp. 139-170, http://dx.doi.org/10.5772/57203.

[35] http://skleac.ciac.jl.cn/english/lessons/secm/secm.html.

[36] http://lektrokeem.blogspot.com/p/blog-page_14.html.

[37] Y.G-Garcia, G.T. Burstein, S. Gonzalez, R.M. Souto: Electrochem. Commun. Vol. 6 (2004), p. 637.

[38] H.S. Isaacs: Corros. Sci. Vol. 29 (1989), p. 3

Electrocatalysts for Hydrogen Energy
10.4028/www.scientific.net/SSP.228

On the Use of the Scanning Electrochemical Microscopy in Corrosion Research
10.4028/www.scientific.net/SSP.228.394

DOI References
[3] J. Izquierdo, L. Martín-Ruíz, B.M. Fernández-Pérez, R. Rodríguez-Raposo, J.J. Santana: J. Electroanal. Chem. Vol. 728 (2014), p.148.
http://dx.doi.org/10.1016/j.jelechem.2014.06.009
[4] J. Izquierdo, G. Bolat, D. Mareci, C. Munteanu, S. González, R.M. Souto: Appl. Surf. Sci. Vol. 313 (2014), p.259.
http://dx.doi.org/10.1016/j.apsusc.2014.05.201
[6] A.R. Zeradjanin, N. Menzel, W. Schuhmann, P. Strasser: Phys. Chem. Chem. Phys. Vol. 16 (2014), p.13741.
http://dx.doi.org/10.1039/C4CP00896K
[7] J. Izquierdo, L. Martín-Ruíz, B.M. Fernández-Pérez, L. Fernández-Mérida, J.J. Santana, R.M. Souto: Electrochim. Acta Vol. 134 (2014), p.167.
http://dx.doi.org/10.1016/j.electacta.2014.04.161
[8] L. Aïnouche, L. Hamadou, A. Kadri, N. Benbrahim, D. Bradai: Electrochim. Acta Vol. 133 (2014), p.597.
http://dx.doi.org/10.1016/j.electacta.2014.04.086
[9] W. Liu, F. Cao, Y. Xia, L. Chang, J. Zhang: Electrochim. Acta Vol. 132 (2014), p.377.
http://dx.doi.org/10.1016/j.electacta.2014.04.044
[10] A.S. Bandarenka, A. Maljusch, V. Kuznetsov, K. Eckhard, W. Schuhmann: J. Phys. Chem. C. Vol. 118 (2014), p.8952.
http://dx.doi.org/10.1021/jp412505p
[11] U.M. Tefashe, M.E. Snowden, P.D. Ducharme, M. Danaie, G.A. Botton, J. Mauzeroll: J. Electroanal. Chem. Vol. 720-721 (2014), p.121.
http://dx.doi.org/10.1016/j.jelechem.2014.03.002
[13] C. Li, L. Li, C. Wang, Y. Zhu, W. Zhang: Corros. Sci. Vol. 80 (2014), p.511.
http://dx.doi.org/10.1016/j.corsci.2013.12.003
[15] E. Martinez-Lombardia, Y. Gonzalez-Garcia, L. Lapeire, I. De Graeve, K. Verbeken, L. Kestens, J.M.C. Mol, H. Terryn: Electrochim. Acta Vol. 116 (2014), p.89.
http://dx.doi.org/10.1016/j.electacta.2013.11.048
[16] A. Maho, F. Kanoufi, C. Combellas, J. Delhalle, Z. Mekhalif: Electrochim. Acta Vol. 116 (2014), p.78.
http://dx.doi.org/10.1016/j.electacta.2013.11.008
[17] S.S. Jamali, S.E. Moulton, D.E. Tallman, M. Forsyth, J. Weber, G.G. Wallace: Corros. Sci. Vol. 86 (2014), p.93.
http://dx.doi.org/10.1016/j.corsci.2014.04.035
[18] X.J. Raj, T. Nishimura: ISIJ International Vol. 54 (3) (2014), p.693.
http://dx.doi.org/10.2355/isijinternational.54.693
[20] R. Moreira, M.K. Schütz, M. Libert, B. Tribollet, V. Vivier: Bioelectrochem. Vol. 97 (2014), p.69.
http://dx.doi.org/10.1016/j.bioelechem.2013.10.003
[21] S. Thomas, I.S. Cole, Y. Gonzalez-Garcia, M. Chen, M. Musameh, JM.C. Mol, H. Terryn, N. Birbilis: J. Appl. Electrochem. Vol. 44 (2014), p.747.

http://dx.doi.org/10.1007/s10800-014-0684-0
[23] M. Serrapede, G. Denuault, M. Sosna, G.L. Pesce, R.J. Ball: Anal. Chem. Vol. 85 (2013), p.8341.
http://dx.doi.org/10.1021/ac4017055
[24] M.B. Jensen, D.E. Tallman: J. Solid State Electrochem. Vol. 17 (2013), p.2999.
http://dx.doi.org/10.1007/s10008-013-2154-8
[25] R.K. Zhu, B.T. Lu, J.L. Luo, Y.C. Lu: Appl. Surf. Sci. Vol. 270 (2013), p.755.
http://dx.doi.org/10.1016/j.apsusc.2013.01.150
[26] L-Å. Näslund, C.M. Sánchez-Sánchez, Á.S. Ingason, J. Bäckström, E. Herrero, J. Rosen, S. Holmin: J. Phys. Chem. C Vol. 117 (2013), p.6126.
http://dx.doi.org/10.1021/jp308941g
[27] A. Davoodi, J. Pan, C. Leygraf, R. Parvizi, S. Norgren: Mater. Corros. Vol. 64 (3) (2013), p.195.
http://dx.doi.org/10.1002/maco.201106466
[28] J. Izquierdo, L. Nagy, S. Gonzàlez, J.J. Santana, G. Nagy, R.M. Souto: Electrochem. Commun. Vol. 27 (2013), p.50.
http://dx.doi.org/10.1016/j.elecom.2012.11.002
[29] G. Bolat, J. Izquierdo, J.J. Santana, D. Mareci, R.M. Souto: Electrochim. Acta Vol. 88 (2013), p.447.
http://dx.doi.org/10.1016/j.electacta.2012.10.026
[30] R.M. Souto, A. Kiss, J. Izquierdo, L. Nagy, I. Bitter, G. Nagy: Electrochem. Commun. Vol. 26 (2013), p.25.
http://dx.doi.org/10.1016/j.elecom.2012.10.001
[31] J. Izquierdo, L. Nagy, I. Bitter, R.M. Souto, G. Nagy: Electrochim. Acta Vol. 87 (2013), p.283.
http://dx.doi.org/10.1016/j.electacta.2012.09.029
[32] A. Pilbáth, T. Szabó, J. Telegdi, L. Nyikos: Prog. Org. Coat. Vol. 75 (2012), p.480.
http://dx.doi.org/10.1016/j.porgcoat.2012.06.006
[33] F. Billi, E. Onofre, E. Ebramzadeh, T. Palacios, M.L. Escudero, M.C. Garcia-Alonso: Surf. Coat. Technol. Vol. 212 (2012), p.134.
http://dx.doi.org/10.1016/j.surfcoat.2012.09.034
[37] Y. G-Garcia, G.T. Burstein, S. Gonzalez, R.M. Souto: Electrochem. Commun. Vol. 6 (2004), p.637.
http://dx.doi.org/10.1016/j.elecom.2004.04.018
[38] H.S. Isaacs: Corros. Sci. Vol. 29 (1989), p.3.
http://dx.doi.org/10.1016/0010-938X(89)90038-3